BMC Research Notes

RESEARCH NOTE Open Access

Impact of different 3D culture environments on spheroid morphology, drug response, and invasion in pancreatic cancer cells

Didem Karakas[1*] and Sila Sigirli[1]

Abstract

Objective Three-dimensional (3D) culture systems offer a more physiologically relevant environment than conventional two-dimensional (2D) cultures, particularly for studying tumor biology. Here, we systematically compared two widely used 3D platforms—poly(2-hydroxyethyl methacrylate) (Poly-HEMA, PH)-coating and ultra-low attachment (ULA) plates—to evaluate their impact on pancreatic cancer (PCa) cell behavior. We assessed spheroid morphology, chemotherapeutic response, invasion potential, and adhesion molecule expression in two PCa cell lines (PANC-1 and SU.86.86).

Results Spheroid morphology differed markedly between PH and ULA platforms, with ULA generally promoting larger and more cohesive spheroids. Gemcitabine resistance was the highest in SU.86.86 spheroids on ULA plates. Matrigel invasion assays revealed enhanced single-cell migration in SU.86.86 spheroids grown on PH, whereas ULA spheroids exhibited broader matrix degradation and collective invasion. Moreover, gene and protein expression levels of key adhesion molecules, including E-Cadherin, N-Cadherin, and integrins, varied between platforms in both cells. These findings demonstrate that 3D culture systems distinctly influence PCa cell characteristics and highlight the necessity of selecting appropriate culture environment for studying tumor biology and drug response. Further mechanistic studies are warranted to uncover how different 3D environments shape tumor cell behavior and therapy resistance.

Keywords 3D culture, Spheroids, Pancreatic cancer, Poly-HEMA, Ultra-low attachment plate

Introduction

Three-dimensional (3D) cell culture systems offer more physiologically relevant in vitro models compared to conventional two-dimensional (2D) cultures, which often fail to replicate the complex architecture and microenvironment of tumors [1–3]. While ultralow-attachment (ULA) plates are commonly used for scaffold-free spheroid formation, their cost may limit broader application [4]. Poly-HEMA (PH) coating has emerged as a more affordable alternative for generating spheroids [5].

During a previous project, we noticed that pancreatic cancer (PCa) spheroid size varied depending on whether cells were cultured on ULA or PH-coated plates. This unexpected observation prompted us to systematically compare these two culture platforms using PANC-1 and SU.86.86 cell lines. Specifically, we assessed spheroid morphology, gemcitabine response, invasion potential, and adhesion molecule expression.

*Correspondence:
Didem Karakas
didem.zeybek@acibadem.edu.tr
[1]Medical Biotechnology, Graduate School of Health, Acibadem Mehmet Ali Aydinlar University, Istanbul, Turkey

© The Author(s) 2025. **Open Access** This article is licensed under a Creative Commons Attribution-NonCommercial-NoDerivatives 4.0 International License, which permits any non-commercial use, sharing, distribution and reproduction in any medium or format, as long as you give appropriate credit to the original author(s) and the source, provide a link to the Creative Commons licence, and indicate if you modified the licensed material. You do not have permission under this licence to share adapted material derived from this article or parts of it. The images or other third party material in this article are included in the article's Creative Commons licence, unless indicated otherwise in a credit line to the material. If material is not included in the article's Creative Commons licence and your intended use is not permitted by statutory regulation or exceeds the permitted use, you will need to obtain permission directly from the copyright holder. To view a copy of this licence, visit http://creativecommons.org/licenses/by-nc-nd/4.0/.

Our results show that the choice of 3D platform markedly alters spheroid formation and drug sensitivity, particularly in SU.86.86 cells. Both cells have bigger and resistant spheroids in ULA plates. Invasive behavior and adhesion molecule expression also varied across platforms. These findings highlight the importance of selecting appropriate 3D culture systems when modeling tumor behavior or testing therapeutic agents in vitro.

Methods

Cell culture

PANC-1 and SU.86.86 PCa cells were purchased from ATCC (Manassas, VA, USA), and BxPC-3 was provided by Dr. Mumin Alper Erdogan (Izmir Katip Celebi University). PANC-1 and BxPC-3 were cultured in high-glucose DMEM, while SU.86.86 was cultured in RPMI-1640, each supplemented with 10% fetal bovine serum (FBS) and 1% penicillin–streptomycin (P/S). Cells were maintained at 37 °C in 5% CO_2 and routinely tested for mycoplasma.

3D culture and spheroid formation

Spheroids were formed using Poly(2-hydroxyethyl methacrylate) (Poly-HEMA, PH)-coated plates or ultra-low attachment (ULA) plates. PH was dissolved in 95% ethanol (20 mg/mL), heated at 65 °C overnight, and added to wells. After air-drying, plates were stored at 4 °C and washed with PBS before use. PCa cells were seeded in PH or ULA plates at 1×10^6 cells/well (6-well) or 3×10^3 cells/well (96-well), then cultured for ≥ 3 days before the experiments.

Gemcitabine treatment and cell viability

Spheroids were treated with gemcitabine (250–4000 µg/ml) for 48 h. Cell viability was assessed by ATP-based cell assay [6]. Luminescence was measured using a 1 s integration time. Experiments were performed in triplicate and repeated at least twice.

Cell invasion assay

PANC-1 and SU.86.86 spheroids (5×10^5 cells) were resuspended in ECM gel (E1270, Sigma-Aldrich) and plated as 20 µL droplets. Following polymerization of ECM, complete medium was added. Images were captured days 0 and 14 using a Zeiss Axiovert 5 inverted fluorescence microscope.

Table 1 Gene names and primary sequences

Gene name	Primer sequences
Glyceraldehyde-3-phosphate dehydrogenase (GAPDH)	F: AGGGCTGCTTTTAACTCTGGT R: CCCCACTTGATTTTGGAGGGA
Cadherin 1 (CDH1) (E-Cadherin)	F: AGTGGGCACAGATGGTGTGA R: TAGGTGGAGTCCCAGGCGTA
Cadherin 2 (CDH2) (N-Cadherin)	F: GCGTCTGTAGAGGCTTCTGG R: GCCACTTGCCACTTTTCCTG
Integrin subunit alpha 1 (ITGA1)	F: GGGAAGCTGCCAGTGAGATT R: GCAGCAGCGTAGAACAACAG
Integrin subunit alpha 5 (ITGA5)	F: CTTCAACTTAGACGCGGAGG R: GCAGGGTGCATACTCCAGAA

Real-time PCR

Cells (1×10^6/well) were cultured for ≥ 3 days. RNA was extracted using the RNeasy Plus Mini Kit (Qiagen), and quality was assessed via NanoDrop 2000. cDNA was synthesized from 500 ng of RNA using iScript™ cDNA Synthesis Kit (Bio-Rad). Quantitative PCR was performed on a Bio-Rad T100 Thermal Cycler. Gene expression was normalized to GAPDH using the ΔΔCt method. Primer sequences are listed in Table 1.

Western blot

Cells were lysed in RIPA buffer supplemented with protease and phosphatase inhibitors. Protein concentrations were determined using the BCA assay (Thermo Fisher Scientific, 23225). Equal amounts of protein (20–30 µg) were loaded onto 10% SDS-PAGE gels and transferred to PVDF membranes (Immobilon®-P, Millipore). Membranes were blocked in 5% non-fat milk in TBS-T and incubated overnight at 4 °C with primary antibodies against E-Cadherin (BD, 610182), N-Cadherin (Invitrogen, 33-3900), and integrin-α5 (Abcam, EPR19669). After washing, membranes were incubated with HRP-conjugated secondary antibodies, and signals were detected using ECL (Bio-Rad) with a ChemiDoc™ MP Imaging System.

Immunofluorescence staining

Spheroids were collected, centrifuged to settle, and fixed in 4% paraformaldehyde for 20 min at room temperature. After washing with PBS, they were permeabilized with 0.3% Triton X-100 in PBS for 20 min and blocked in 3% BSA/0.1% Triton X-100 for 1 h. Spheroids were incubated with primary antibodies (E-Cadherin, Integrin α1; 1:250 in blocking buffer) overnight at 4 °C with gentle agitation, washed three times for 10 min in PBS/0.1% Tween-20, and subsequently incubated with Alexa Fluor–conjugated secondary antibodies (1:500) for 1 h at room temperature in the dark. Nuclei were counterstained with DAPI (1 µg/mL, 10 min). Spheroids were transferred to glass-bottom dishes, mounted in antifade medium, and imaged using a confocal microscope.

Quantification of immunofluorescence staining was performed using FIJI (ImageJ). For each spheroid, mean fluorescence intensity (MFI) was measured from manually defined ROIs under identical acquisition settings. Background signal was subtracted from cell-free regions of the same image. At least four images per condition were analyzed. Quantitative data are presented as mean ± SEM. Differences between PH vs. ULA grown spheroids were analyzed using an unpaired two-tailed

t-test with Welch's correction to account for potential unequal variances. Statistical analyses were performed using GraphPad Prism (v10, GraphPad Software, San Diego, CA, USA). A $p < 0.05$ was considered statistically significant.

Statistical analysis

Data are presented as mean ± SD or fold change. Statistical significance was assessed using Student's t-test or one-/two-way ANOVA in GraphPad Prism 9.0. Significance levels were indicated as $^{*}p < 0.05$, $^{**}p < 0.01$, $^{***}p < 0.001$, $^{****}p < 0.0001$.

Results

Spheroid morphology and basal proliferation differ between culture platforms

All three PCa cell lines formed spheroids with distinct morphological features depending on the culture platform. PH-coated plates yielded smaller, less cohesive spheroids, while ULA plates promoted significantly larger and more compact structures (Fig. 1A, B). To compare basal proliferation, ATP-based viability assays were performed after 5 days in culture. Baseline ATP levels (RLUs) were consistently lower in ULA-grown cells than in PH-grown counterparts across all lines, suggesting reduced metabolic activity under ULA conditions (Fig. 1C).

PCa cells exhibit differential responses to gemcitabine depending on the culture platforms

Following morphological and metabolic differences, we aimed to evaluate drug sensitivity therefore, PANC-1 and SU.86.86 spheroids were treated with gemcitabine (0.125–4000 µg/mL) for 48 h. BxPC-3 was excluded due to minimal differences in earlier assays. PANC-1 cells showed minimal differences between platforms, except at the highest dose, where PH-cultured spheroids had lower viability (Fig. 2A). In contrast, SU.86.86 spheroids grown on ULA plates were notably more resistant across all doses (Fig. 2B).

Annexin-V staining confirmed apoptotic activity in all treated groups. Spheroid disruption was evident in PH-cultured PANC-1 and SU.86.86 cells at high doses, whereas ULA spheroids remained more intact, indicating platform-dependent structural resilience (Fig. 2C, D).

Invasion potential and adhesion marker expression vary by culture platform

To evaluate invasion potential, PANC-1 and SU.86.86 spheroids grown on PH-coated or ULA plates were embedded in ECM and cultured for 2 weeks. PANC-1 spheroids largely remained intact within the matrix, with limited ECM degradation observed in PH-derived spheroids (Fig. 3A). In contrast, SU.86.86 spheroids showed greater invasion, especially those initially grown on PH plates (Fig. 3B). Phenotypically, SU.86.86 spheroids

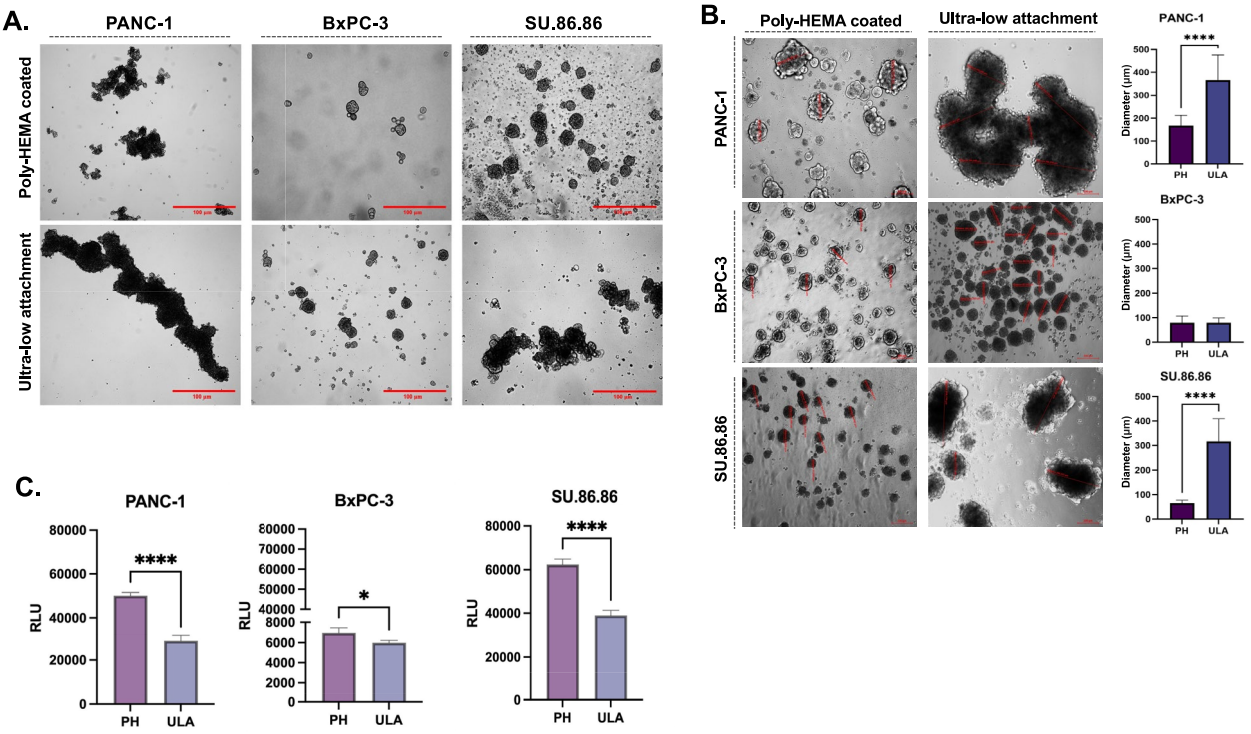


Fig. 1 Spheroid morphology and basal proliferation varies between culture platforms. Morphological (**A**) and size (**B**) differences in spheroids in PH-coated or ULA plates. PCa cells grown on ULA plates exhibited lower ATP levels across all cell types (**C**). $^{*}p < 0.05$, $^{****}p < 0.0001$. RLU; relative light units

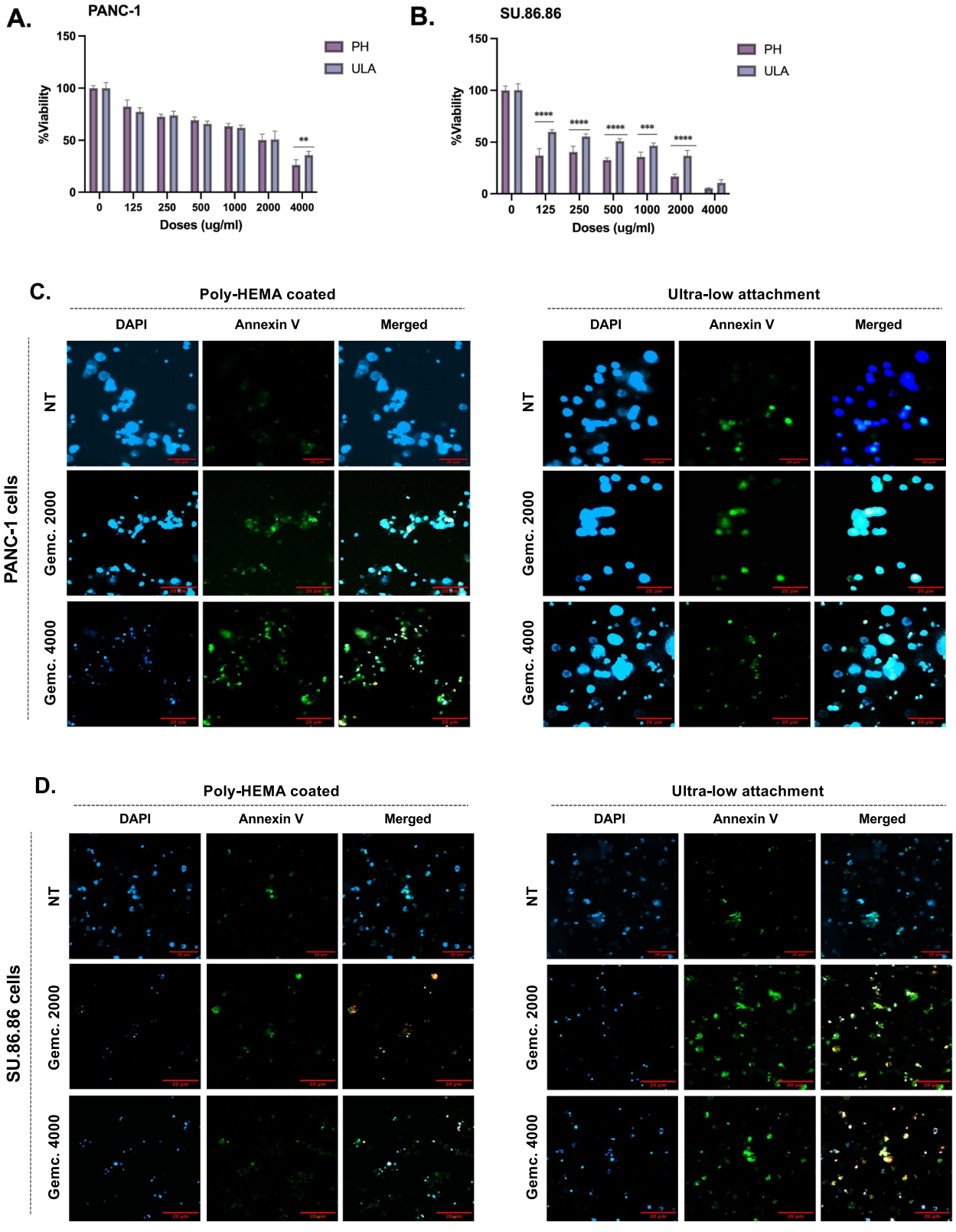


Fig. 2 Gemcitabine response varies with 3D culture platform. PANC-1 spheroids showed no significant differences between PH and ULA conditions, except at the highest dose (**A**). SU.86.86 spheroids were significantly more sensitive to gemcitabine when cultured on ULA plates, particularly at lower doses (**B**). In both cell lines, Annexin positivity was observed in gemcitabine-treated groups. Spheroid disruption was more pronounced in PH-cultured cells at high doses, whereas spheroids cultured in ULA plates largely retained their structural integrity. Panel C shows representative images from PANC-1 cells, and panel D from SU.86.86 cells (**C**, **D**). *$p < 0.05$, **$p < 0.01$, ***$p < 0.001$, ****$p < 0.0001$

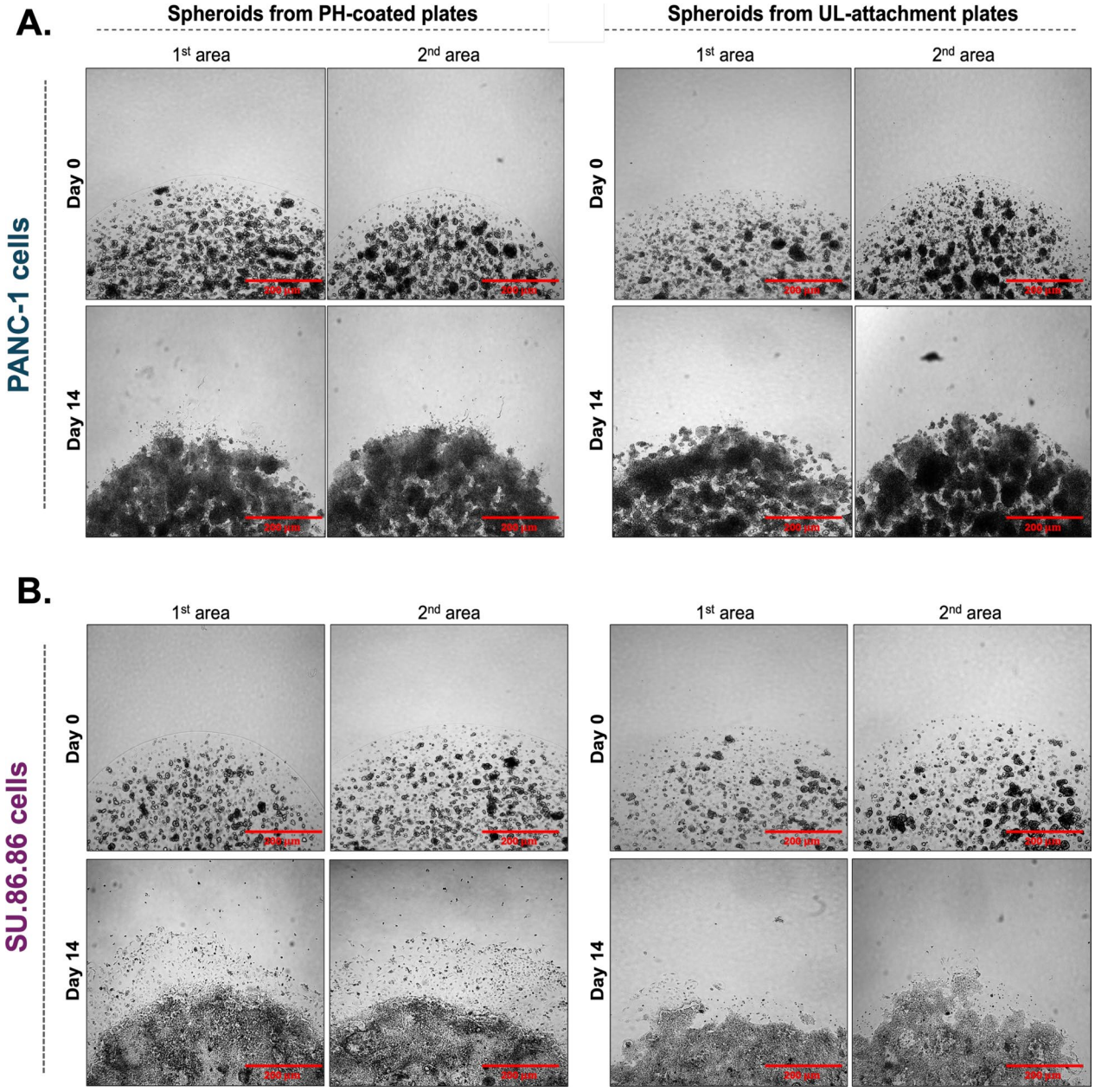


Fig. 3 Cell invasion differs by culture platform. PANC-1 spheroids largely remained within the ECM, with only slight degradation observed in PH-derived spheroids (**A**). In contrast, SU.86.86 spheroids exhibited more pronounced invasion when derived from PH plates, whereas ULA cultures induced broader ECM degradation (**B**)

derived from PH showed more single-cell invasion, whereas ULA-derived spheroids caused broader matrix degradation, indicating distinct invasion patterns driven by the culture platform.

Adhesion molecule profiling revealed platform- and cell type-dependent differences. In PANC-1 spheroids, N-Cadherin and MMP-7 mRNA expression was higher on PH, whereas E-Cadherin protein expression was elevated on ULA despite lower transcript levels (Fig. 4A). Integrin α5 expression remained unchanged, while integrin α1 (ITGA1) mRNA was increased under ULA conditions (Fig. 4A).

In SU.86.86 spheroids, N-Cadherin protein levels were slightly higher in PH cultures, while its mRNA levels were higher under ULA conditions, suggesting post-transcriptional regulation. Integrin α1 and MMP-7 mRNA levels were also higher in ULA spheroids (Fig. 4B). While SU.86.86 cells on PH exhibited more individual cell invasion, ULA-derived spheroids caused broader matrix degradation, indicating distinct invasion patterns driven by culture platform.

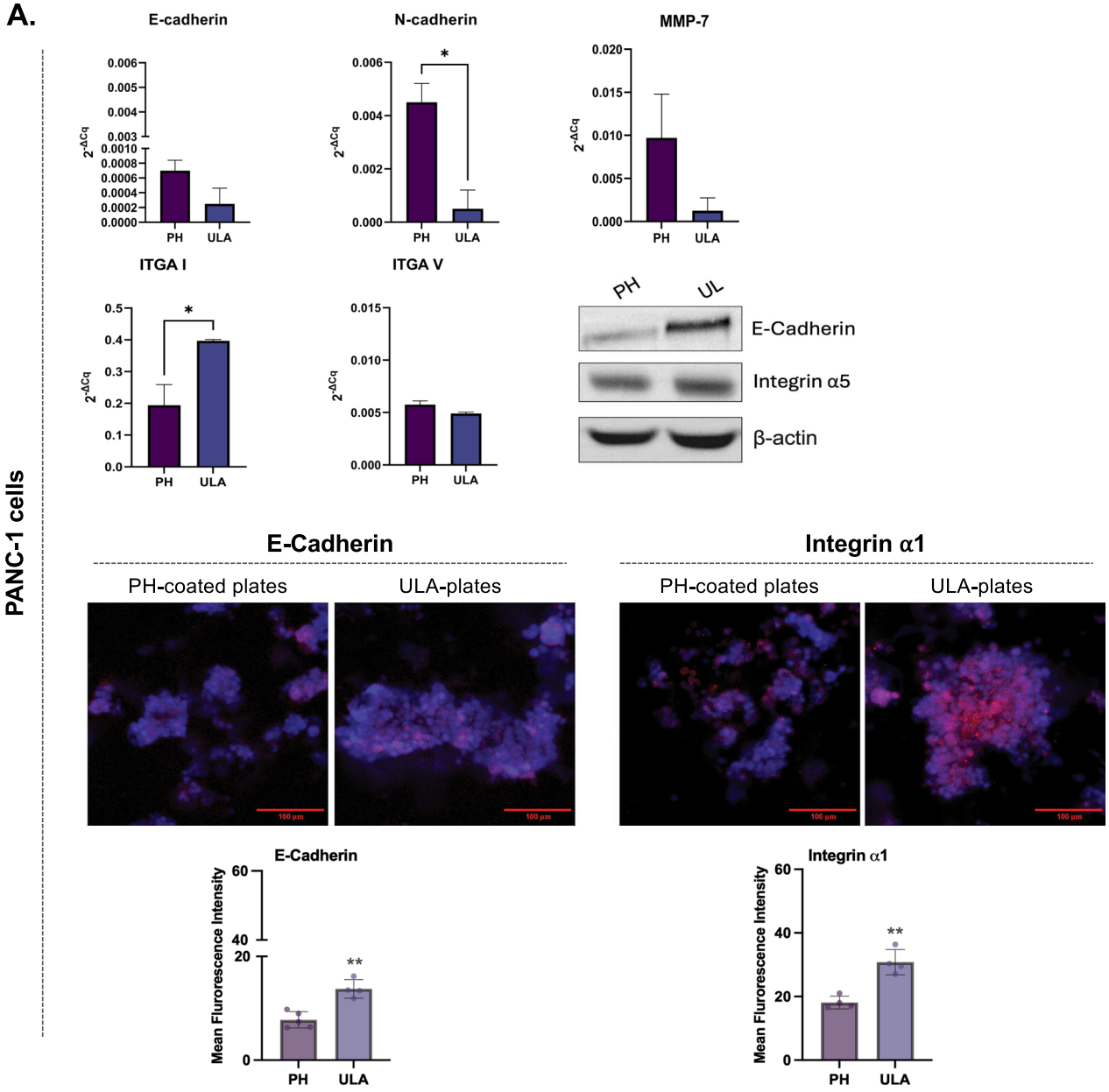


Fig. 4 Platform-dependent differences in adhesion and invasion marker expression. In PANC-1 spheroids, E-Cadherin protein expression was higher under ULA conditions, while N-Cadherin and MMP-7 mRNA levels were elevated in PH cultures. Integrin α1 and MMP-7 mRNA were increased in ULA spheroids. Representative immunofluorescence staining further confirmed higher E-Cadherin and Integrin α1 expression in ULA cultures (**A**). In SU.86.86 cells, N-Cadherin protein expression was higher in PH, but its mRNA levels, together with MMP-7 and Integrin α1, were elevated in ULA. Immunofluorescence staining confirmed these trends (**B**). *$p < 0.05$, **$p < 0.01$, ***$p < 0.001$, ***$p < 0.0001$. Bottom panels show quantitative mean fluorescence intensity (MFI) analysis of E-Cadherin and Integrin α1 from ≥ 4 images per group. Data are mean ± SEM; *$p < 0.05$, **$p < 0.01$ (unpaired t-test)

Quantitative analysis of immunofluorescence staining further confirmed these observations. In PANC-1 spheroids, mean fluorescence intensity (MFI) of E-Cadherin was significantly higher in ULA cultures compared with PH (13.7 vs. 7.8), consistent with protein data. Similarly, Integrin α1 MFI was markedly elevated in ULA spheroids (30.8 vs. 18.1). In SU.86.86 spheroids, differences were more modest but followed a similar trend: slightly higher E-Cadherin and Integrin α1 intensities were observed under PH conditions (E-Cadherin: 38.5 vs. 30.6; Integrin α1: 41.6 vs. 39.0), consistent with their more scattered invasion phenotype. Interestingly, integrin α1 staining intensity in ULA spheroids was lower than expected from mRNA data, further supporting that transcript levels do not always directly correlate with protein abundance.

Discussion

3D culture systems offer more physiologically relevant models than traditional 2D monolayers by better mimicking the tumor and its microenvironment [2, 7, 8]. Among scaffold-free platforms, PH-coated surfaces and ULA plates are commonly used for spheroid formation. PH, a non-adherent polymer, offers cost-effectiveness and flexibility, while ULA surfaces prevent adhesion via hydrophilic polymer coatings [9, 10]. Although many studies are available using these platforms, their impact on PCa cell behavior has not been comprehensively compared.

Here, we assessed how these platforms influence spheroid formation, drug response, invasion, and adhesion-related gene/protein expression in PCa cell lines. Spheroid structure varied with both cell line and culture platform. PH yielded smaller, compact spheroids, whereas ULA plates promoted more cohesive structures. These differences likely reflect the epithelial or mesenchymal origin of the cells: PANC-1 formed cohesive spheroids in our setting, yet the literature describes PANC-1 as partial-EMT/mesenchymal-leaning with low E-Cadherin and reduced tight junction markers (e.g., ZO-1, occludin), suggesting that cohesion likely reflects platform-dependent cell–cell interactions and actomyosin-driven compaction rather than mature epithelial junctions [11]. In contrast, SU.86.86 cells formed grape-like structures, whereas BxPC-3 cells developed small, compact, and well-defined spheroids, consistent with previous 3D culture observations [12].

We observed greater gemcitabine resistance in 3D cultures than in 2D, aligning with the literature. In 3D culture, SU.86.86 on ULA plates showed the highest resistance, whereas PANC-1 exhibited only minor platform-dependent differences. The distinct behaviors—particularly in SU.86.86 cells—may arise from platform-specific microenvironments that differentially modulate gene expression, protein stability/localization, and biomechanical cues [13–15].

Invasion phenotypes were likewise platform-dependent. PANC-1 spheroids remained largely confined regardless of the platform, showing only slight invasive potential when grown on PH plates. E-Cadherin protein expression was elevated in ULA cultures, despite lower mRNA levels, suggesting post-transcriptional regulation. Conversely, N-Cadherin mRNA was higher in PH cultures, correlating with slightly increased invasive behavior. SU.86.86 spheroids, however, showed pronounced invasion, especially when derived from PH-coated plates, displaying dispersed single-cell migration. In contrast, ULA-grown spheroids demonstrated broader matrix degradation with more collective behavior. Adhesion marker profiling revealed a complex, platform-dependent pattern in SU.86.86 spheroids. N-Cadherin protein expression was slightly higher in PH cultures, consistent with their more migratory phenotype, whereas MMP-7 mRNA levels were significantly elevated in ULA spheroids, suggesting a post-transciptional regulation. Integrin α1 gene expression was also higher in ULA spheroids, which may contribute to enhanced cell–ECM adhesion and support the collective invasion pattern characteristic of these cultures.

Quantitative analysis of immunofluorescence staining across multiple spheroids further supported these findings. Significantly higher E-Cadherin and integrin α1 intensities were detected in PANC-1 spheroids under ULA conditions, whereas SU.86.86 spheroids displayed slightly higher intensities under PH conditions. These quantitative data corroborate our Western blot results and strengthen the conclusion that culture platform strongly influences adhesion molecule expression profiles.

Interestingly, we observed instances where mRNA and protein levels were not aligned, and in some cases showed opposite trends (e.g., integrin α1 in SU.86.86 spheroids). This is biologically plausible: post-transcriptional regulation via microRNAs, RNA-binding proteins, and translational control can uncouple transcript levels from protein output. In addition, protein half-life, post-translational modifications, and trafficking may dictate final protein abundance independent of transcription [16–19]. For example, integrin α1 mRNA upregulation under ULA conditions in SU.86.86 may not translate to higher protein levels if protein turnover is rapid.

MicroRNAs provide an additional regulatory layer that can decouple transcript levels from protein output. Global analyses have shown that microRNAs can reduce protein abundance either by promoting mRNA destabilization or by repressing translation without affecting mRNA abundance [20]. In addition, mRNA and protein differ markedly in synthesis and degradation kinetics: transcripts are generally short-lived (minutes), whereas proteins can persist for hours to days, and these rates are often uncorrelated for the same gene [21]. Consequently, a direct correlation between mRNA and protein levels is rarely observed, underscoring the need to complement transcriptomic data with protein-level validation [22].

MMP-7 expression also showed platform-specific differences: in SU.86.86 cells, MMP-7 mRNA was significantly higher in ULA spheroids, which exhibited broader matrix degradation. Given that MMP-7 facilitates invasion by degrading ECM and cleaving cell adhesion molecules such as E-Cadherin [23, 24], its upregulation may promote tissue remodeling and invasion in dense spheroids. In PANC-1 cells, MMP-7 expression was modestly higher in PH conditions, aligning with localized ECM degradation and release of invasive cells. Interestingly, although MMP-7 levels were elevated in ULA-grown SU.86.86 spheroids, these cells displayed more

pronounced single-cell migration when cultured on PH. This observation suggests that different proteolytic programs may drive distinct invasion modes, with MMP-7 potentially contributing more to collective ECM remodeling in ULA spheroids, while other MMPs (e.g., MMP-2, MMP-9) may facilitate individual cell invasion in PH conditions.

Cell-line-specific differences might also influence their response to different platforms. PANC-1, established from a 56-year-old male with primary PDAC, is often described as epithelial in morphology but shows EMT-leaning, mesenchymal-like expression (low E-Cadherin, high vimentin) and context-dependent migratory potential [25]. SU.86.86 cells, derived from a 57-year-old female with pancreatic adenocarcinoma (liver metastasis reported), are commonly categorized as epithelial-like yet displays marked plasticity. We therefore used these two lines to sample distinct positions along the epithelial–mesenchymal spectrum and to test whether PH vs ULA microenvironments differentially shape spheroid architecture, invasion modes, and drug sensitivity.

Taken together, these data suggest that PANC-1 cells, which are more epithelial-like, respond to ULA conditions by stabilizing cell–cell junctions and maintaining a cohesive phenotype, whereas SU.86.86 cells respond to PH by adopting a more migratory program with single-cell invasion. This highlights how intrinsic differences between cell lines interact with culture conditions to yield distinct phenotypes.

Our findings suggest that ULA plates are particularly suitable for studies focusing on epithelial-like phenotypes and drug resistance, while PH-coated plates may be preferable for capturing EMT-related phenotypes and single-cell invasion. For drug screening, ULA consistently produced larger, structurally resilient spheroids and higher gemcitabine resistance—most notably in SU.86.86—supporting ULA-based workflows when the goal is to capture chemoresistant, mechanically stable phenotypes. For invasion/EMT-oriented studies, PH generated smaller, less cohesive spheroids and exposed single-cell migration more readily in SU.86.86, whereas ULA favored broader ECM degradation and collective components. Thus, platform choice should be carefully matched to the biological question, and combined transcript–protein readouts are recommended for mechanistic interpretation.

Limitations

This study is limited by the use of only two PCa cell lines for functional comparisons, which may not fully capture the heterogeneity of the disease. Additionally, gene and protein expression analyses were restricted to selected adhesion and invasion markers; broader transcriptomic or proteomic profiling could provide deeper mechanistic insights. Another limitation is the partial mismatch observed between transcript and protein levels for certain markers, as not all mRNA changes could be validated at the protein level, and vice versa. This may reflect biological regulation but also highlights the need for multi-omics approaches to achieve a more integrated understanding. Moreover, other potentially informative spheroid parameters, such as circularity and the total number of spheroids formed from a given seeding density, were not assessed in the present study and warrant further investigation. Finally, while in vitro 3D models offer improved physiological relevance compared to 2D cultures, they still lack stromal and immune components present in the native tumor microenvironment.

Acknowledgements
We used ChatGPT 4o (OpenAI, 2025) for minor language editing and sentence restructuring support during manuscript preparation.

Author contributions
Investigation, conceptualisation, methodology, writing—original draft, visualisation, supervision, D.K.; writing, review, and editing. S.S. and D.K. All authors have read and agreed to the published version of the manuscript.

Funding
This research received no external funding.

Data availability
All data generated or analyzed during this study are included in this published article. This study does not involve any of the data types listed under BMC's mandatory data deposition policy (e.g., sequencing, proteomics, genomics, or functional genomics datasets); therefore, no accession numbers are applicable.

Declarations

Ethics approval and consent to participate
Not applicable.

Consent for publication
Not applicable.

Competing interests
The authors declare no competing interests.

Received: 11 June 2025 / Accepted: 25 September 2025
Published online: 28 October 2025

References

1. Breslin S, O'Driscoll L. Three-dimensional cell culture: the missing link in drug discovery. Drug Discov Today. 2013;18(5–6):240–9.
2. Ravi M, Paramesh V, Kaviya SR, Anuradha E, Paul Solomon FD. 3D cell culture systems: advantages and applications. J Cell Physiol. 2015;230(1):16–26.
3. Yamada KM, Cukierman E. Modeling tissue morphogenesis and cancer in 3d. Cell. 2007;130(4):601–10.
4. Vinci M, Gowan S, Box C, et al. Advances in establishment and analysis of three-dimensional tumor spheroid-based functional assays for target validation and drug evaluation. BMC Biol. 2012;10(1):29.
5. Kim SH, Turnbull J. Formation of chondrogenic spheroids using poly-HEMA in chemically defined conditions. Biomaterials. 2011;32(9):2451–9.
6. Karakas D, Cevatemre B, Aztopal N, Ari F, Yilmaz VT, Ulukaya E. Addition of niclosamide to palladium(II) saccharinate complex of terpyridine results in enhanced cytotoxic activity inducing apoptosis on cancer stem cells of breast cancer. Bioorg Med Chem. 2015;23(17):5580–6.

7. Chitcholtan K, Asselin E, Parent S, Sykes PH, Evans JJ. Differences in growth properties of endometrial cancer in three-dimensional (3D) culture and 2D cell monolayer. Exp Cell Res. 2013;319:75–87.
8. Fennema E, Rivron N, Rouwkema J, van Blitterswijk C, de Boer J. Spheroid culture as a tool for creating 3d complex tissues. Trends Biotechnol. 2013;31(2):108–15.
9. Costa EC, de Melo-Diogo D, Moreira AF, Carvalho MP, Correia IJ. Spheroids formation on non-adhesive surfaces by liquid overlay technique: considerations and practical approaches. Biotechnol J. 2018. https://doi.org/10.1002/biot.201700417.
10. Wanigasekara J, Carroll LJ, Cullen PJ, Tiwari B, Curtin JF. Three-dimensional (3D) in vitro cell culture protocols to enhance glioblastoma research. PLoS ONE. 2023;18(2):e0276248.
11. Polireddy K, Dong R, McDonald PR, Wang T, Luke B, Chen P, et al. Targeting epithelial-mesenchymal transition for identification of inhibitors for pancreatic cancer cell invasion and tumor spheres formation. PLoS ONE. 2016;11(10):e0164811.
12. Longati P, Jia X, Eimer J, et al. 3D pancreatic carcinoma spheroids induce a matrix-rich, chemoresistant phenotype offering a better model for drug testing. BMC Cancer. 2013;13:95.
13. Ben-David U, Siranosian B, Ha G, Tang H, Oren Y, Hinohara K, et al. Genetic and transcriptional evolution alters cancer cell line drug response. Nature. 2018;560(7718):325–30.
14. Ponce LV, Barrera RR. Changes in P-glycoprotein activity are mediated by the growth of a tumour cell line as multicellular spheroids. Cancer Cell Int. 2005;5:20.
15. Wen Z, Liao Q, Hu Y, You L, Zhou L, Zhao Y. A spheroid-based 3-D culture model for pancreatic cancer drug testing, using the acid phosphatase assay. Braz J Med Biol Res. 2013;46:634–42.
16. Greenbaum D, Colangelo C, Williams K, et al. Comparing protein abundance and mRNA expression levels on a genomic scale. Genome Biol. 2003;4:117.
17. Koussounadis A, Langdon S, Um I, et al. Relationship between differentially expressed mrna and mrna-protein correlations in a xenograft model system. Sci Rep. 2015;5:10775.
18. Vogel C, Marcotte E. Insights into the regulation of protein abundance from proteomic and transcriptomic analyses. Nat Rev Genet. 2012;13:227–32.
19. Wang D. Discrepancy between mRNA and protein abundance: insight from information retrieval process in computers. Comput Biol Chem. 2008;32(6):462–8.
20. Baek D, Villén J, Shin C, Camargo FD, Gygi SP, Bartel DP. The impact of micrornas on protein output. Nature. 2008;455(7209):64–71.
21. Schwanhäusser B, Busse D, Li N, Dittmar G, Schuchhardt J, Wolf J, Chen W, Selbach M. Global quantification of mammalian gene expression control. Nature. 2011;473:337–42. Erratum in: Nature. 2013;495:126–7.
22. Waldbauer JR, Rodrigue S, Coleman ML, Chisholm SW. Transcriptome and proteome dynamics of a light-dark synchronized bacterial cell cycle. PLoS ONE. 2012;7:e43432.
23. Ii M, et al. Matrix metalloproteinase-7 cleaves E-cadherin and promotes cell invasion. Ann Surg. 2006;244(6):928–39.
24. Wang F, Weaver VM, Petersen OW, Larabell CA, Dedhar S, Briand P, et al. Reciprocal interactions between beta1-integrin and epidermal growth factor receptor in three-dimensional basement membrane breast cultures: a different perspective in epithelial biology. Proc Natl Acad Sci U S A. 1998;95:14821–6.
25. Shichi Y, Sasaki N, Michishita M, Hasegawa F, Matsuda Y, Arai T, et al. Enhanced morphological and functional differences of pancreatic cancer with epithelial or mesenchymal characteristics in 3D culture. Sci Rep. 2019;9(1):10871.

Publisher's Note

Springer Nature remains neutral with regard to jurisdictional claims in published maps and institutional affiliations.